High-Throughput Screening Devices Based on Hydrophobic Microfluidics

J.J. Chen, H.J. Yang, J.W. Wu, S.H. Parng and T.M. Yu

Medical Electronics and Device Technology Center, Industrial Technology Research Institute, Hsinchu, Taiwan, R.O.C., Chaucer@itri.org.tw

ABSTRACT

In this work, we develop a microfluidic assay for determination of the individual cell's response to chemical exposure. Microfluidic chips comprised four channels are fabricated on polystyrene (PS) substrates via mechanical milling processes, and covered by polydimethylsiloxane (PDMS) plates. This chip is designed to provide an evenly distributed flow to each perfusion channel and to assure the success of the liquid filling processes. The fabricated chips are characterized by using commercial ink and/or distilled water to see the bubbles progressing along the channels. The blue ink slugs are injected into the bubbles to demonstrate the high-throughput drug screening process. All the blue ink slugs progress down the channels successfully without any dilutions with the liquid water. In the future, this apparatus will serve as a tool for biochemical analyses.

Keywords: microfluidic assay, evenly distributed, bubbles progressing, high-throughput, biochemical analyses

1 INTRODUCTION

During last decades, many efforts were made to improve drug screening technology to identify new drugs among various chemical substances and increase the already acknowledged impact of drug screening technique in the pharmacological field. In this way, the combination of screening technology and microfabrication allowed developing new classes of diagnostic tools with a great interest through cost reductions and fast diagnostics. Tanaka et al. [1] developed a multi-channels drug response assay system on microchips. Several micro syringe pumps were utilized to drive the reagent solutions into the microchips. Puntambekar et al. [2] proposed an air-driven multiplexer integrated with micro dispensers. The dispensed volume was precisely multiplexed into constant volumes of each channel. Only one syringe pump was utilized and hydrophobic microfluidics was a method to control fluid flow in microchannels. In micro-scale system, the flow characteristics in channels show some differences due to the larger surface-to-volume ratio compared to those in the macro system. One of the most well-known phenomena is the fluid-surface interaction which is usually ignored in macro-scale systems. The microfluidic technologies based on surface tension are of several advantages, such as lower power consumption, simple machining and no moving part. Among these technologies hydrophobic valves [3] has been developed with special geometric designs of microchannels [4] or based on wetting patterns [5] for a few years. The objective of the present study is to develop a microfluidic assay for determination of the individual cell's response to chemical exposure. Microfluidic chips comprised four channels are fabricated on polystyrene (PS) substrates via mechanical milling processes, and covered by polydimethylsiloxane (PDMS) plates. Some short geometrical restrictions are placed at the upstream and downstream portions of each flow branch. Hydrophobic valves are used to ensure a sample being evenly distributed. The liquid filling processes in the microfluidic chips are revealed, and the progressing of the bubbles along the channels is demonstrated. Finally, we show the simulated high-throughput drug screening process.

2 THEORY

The hydrophobic valve and capillary filling can be explained in terms of energy changes in the solid-liquid-gas interface system [5]. The total interfacial energy of the system, U_T, can be written as follows,

$$U_T = \sum_{i,j,k} \left(A_{SjLi}\gamma_{SjLi} + A_{SjGk}\gamma_{SjGk} + A_{LiGk}\gamma_{LiGk} \right) \quad (1)$$

where A_{SjLi}, A_{SjGk} and A_{LiGk} are solid-liquid, solid-gas and liquid-gas interface areas, respectively, and γ_{SjLi}, γ_{SjGk} and γ_{LiGk} are their corresponding surface energies per unit area. The relation between the surface energies and the liquid contact angle θ_c at the solid-liquid-gas interface line is expressed in Young's equation as

$$\gamma_{SjGk} = \gamma_{SjLi} + \gamma_{LiGk}\cos\theta_c \quad (2)$$

With the increase of the volume V_L of injected liquid, wetted area is increased and the total energy U_T is a function of the volume V_L. Introducing Eq. (2) into Eq. (1) and the capillary pressure of liquid in a microchannel can expressed as

$$P = -\frac{dU_T}{dV_L} = \sum_{i,j,k} \gamma_{LiGk} \left(\cos\theta_c \frac{dA_{SjLi}}{dV_L} - \frac{dA_{LiGk}}{dV_L} \right) \quad (3)$$

In uniform channels with contact angle less than or equal to 90°, A_{LiGk} is fixed and A_{SjLi} increases linearly with penetration distance. Therefore the liquid wicks in and wets the entire channel surface with a positive capillary pressure which drives the flow. For a microchannel of the rectangle cross-section with the specific width and height, the channel cross-section varies from the narrower to the wider, the geometry of the channel is manipulated in order

to make the capillary pressure become negative, shown in Fig. 1. This can be accomplished for contact angle less than or equal to 90° by an abrupt enlargement in the channel cross section. This enlargement forces A_{LiGk} to increase more than A_{SjLi} for a given volume change resulting in a negative opposing pressure. So the capillary pressure can be expressed as

$$P = -\frac{dU_T}{dV_L} = \gamma_{LG}\left(\cos\theta_c \frac{dA_{SL}}{dV_L} - \frac{dA_{LG}}{dV_L}\right) \quad (4)$$

When the meniscus expands into the wedge region, it results in

$$U_T = U_0 - \gamma_{LG}\left[2wl + 2\left(\frac{x}{\cos\beta}\right)w\right]\cos\theta_c + \frac{(h + 2x\tan\beta)\alpha w\gamma_{LG}}{\sin\alpha} \quad (5)$$

and

$$V_L = wlh + (h + x\tan\beta)wx + \frac{w(h + 2x\tan\beta)^2}{4\sin\alpha}\left(\frac{\alpha}{\sin\alpha} - \cos\alpha\right) \quad (6)$$

where $U_0 = (A_{SL} + A_{SG})\gamma_{SG}$, w and h are the width and height, respectively, of the channel at cross-section, l is the penetration distance before the meniscus entering the enlargement region, x is the penetration distance after the meniscus entering the enlargement region, α is the discontinuity in the channel angle, and β is wedge angle. Substituting Eq. (5) and (6) into Eq. (4), the capillary pressure can be expressed as

$$P = \frac{2\gamma_{LG}}{h}\left[\frac{\cos\theta_c - \frac{\alpha}{\sin\alpha}\sin\beta}{\cos\beta + \frac{\sin\beta}{\sin\alpha}\left(\frac{\alpha}{\sin\alpha} - \cos\alpha\right)}\right] + \frac{2x}{h}\left[\sin\beta + \tan\beta\frac{\sin\beta}{\sin\alpha}\left(\frac{\alpha}{\sin\alpha} - \cos\alpha\right)\right] \quad (7)$$

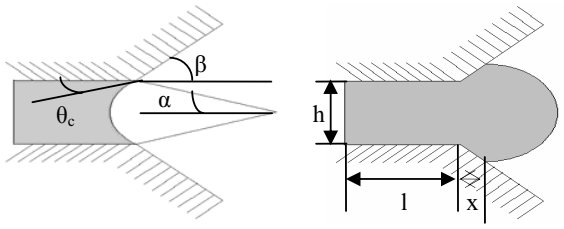

Figure 1: Schematic of the hydrophobic valving.

When the wedge angle is equal to 90° , α is equal to θ_c. The expression of maximum pressure difference between the liquid meniscuses when the meniscus reaches the wedge, according to Eq. (7), can expressed to a reduced form and shown as follows [6],

$$\Delta p = \frac{2\gamma_{LG}\sin\theta_c}{h} \quad (7)$$

A microchannel is maintained in the valve-close state if an external pressure is less than the maximum pressure resulting from Eq. (7). To turn the microchannel to a valve-open state against the liquid flow, the external pressure has to be higher than the maximum pressure needed to push the fluid in a desired direction.

3 EXPERIMENT

Microfluidic chips comprised four channels are fabricated in polystyrene (PS) substrates via mechanical milling processes, and covered by polydimethylsiloxane (PDMS) plates. Figure 2 expresses the completed microchip (100mm x 50mm). This chip is designed as a symmetric channel network with binary splitting so as to provide an evenly distributed flow to each perfusion channel, and the channels are 1mm wide. The bottom of the walls with semi-circle cross section is made to prevent a small amount of liquid moving ahead of the main streams.

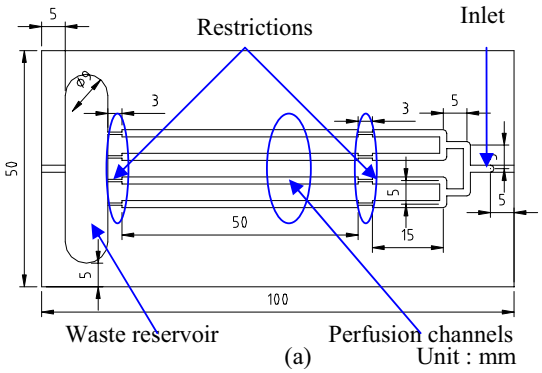

(a)

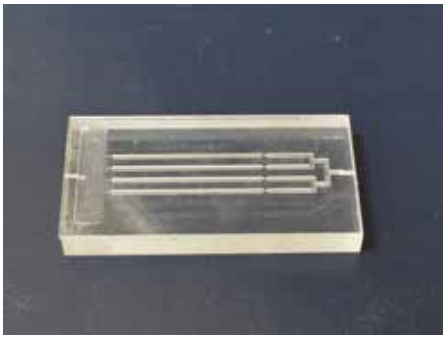

(b)

Figure 2: Completed microfluidic chip: (a) a schematic illustration; (b) the fabricated microfluidic chip.

Lago and Araujo [7] reported that the capillary pressure will not be decreased when the wall curve for the capillary

cross section is circle. It means the wetting fluid cannot be located in the crevices and wedges of the capillary, and thus, in processes such as drainage, the wetting fluid may not remain connected and flow through films. Therefore, a small amount of liquid will not move ahead of the main streams along the crevices. Some short geometrical restrictions are placed at the upstream and downstream portions of each flow branch, and the widths of the restrictions are 0.5mm. Besides we make a large waste reservoir at the end of these channels. The hydrophobic valves are introduced and the pressure barrier is developed when cross section of channels changes abruptly in the restriction regions. These can assure the success of the liquid filling processes.

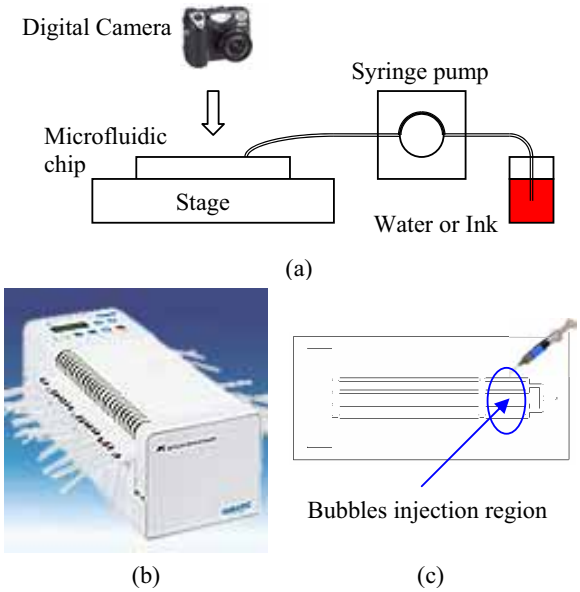

Figure 3: Schematic illustrations of (a) the entire experimental setup, (b) the apparatus for liquid sample injection, and (c) the generation of air bubbles.

The culture medium is delivered into the inlet channel by one syringe pump. Figure 3 shows a schematic illustration of the entire experimental setup. The microfluidic chip is placed and fixed on a stage. The apparatus is designed to execute liquid sample injection. As shown in Fig. 3(b), the apparatus consists of a full set of syringes pump (IP-N 24, ISMATEC), and the flow rates per channel of this pump are range from 0.0004~11ml/min. The sample is injected through Tygon microbore tubing plastic tubes, which are connected to the microchip. After finishing the filling processes, the bubbles are injected at the locations between the starting point of the channels and the restrictions sequentially, shown in Fig. 3(c). Then drug slugs are introduced into the bubbles; and the dilutions of drugs with the culture medium can be avoided. When the pump starts, the drugs flow passing the cells spread onto the bottoms of the channels. Therefore the screening processes are finished. A digital camera (Coolpix 5000, Nikon) is used to snap the moving of the liquid-gas interface.

4 RESULTS AND DISCUSSION

In the follows, we consider the configuration of the flow network system. The microchannels are with the width of 1mm for the overall microfluidic system. The restrictions are with the width of 0.5mm. In the following, the liquid filling processes in the microfluidic chips are shown, and the bubbles and liquid slugs progressing along the channels are also revealed.

In Figures 4 to 6, as a cover under which the micro system is fabricated in polystyrene (PS) substrates by mechanical milling processes, we have selected the polydimethylsiloxane (PDMS) plates, which is nearly transparent in the visible light spectrum. Flow experiments are performed more than three times, under the same condition, to check the repeatability. We showed four snap shots of the liquid filling processes in the microfluidic chips in Fig. 4. The medium enters into the inlet channel with the pumping velocity equal to 200μl/min. The medium flow proceeds forward and approaches the entrance of the perfusion channels. One of the meniscuses stops as it reaches the upstream restriction. Then other gas-liquid interfaces proceed and stop consecutively. After the pressure barriers are overcome, one meniscus continues further down the channels and stops when it reaches the downstream restriction. Furthermore all the interfaces reach the restrictions; thus the medium flows into the waste reservoir without any bubble entrapments.

Figure 4: Photos of the liquid filling process for four consecutive times.

To see the bubbles progressing along the channels, the fabricated chips are characterized by using commercial ink and/or distilled water. In Fig. 5, it illustrats that the bubbles are generated by syringe needles and move along the channels which are filled with the red ink. And then the red ink is introduced from the inlet again. The interfaces stop at

the restrictions successively, and then the bubbles moving processes are finished.

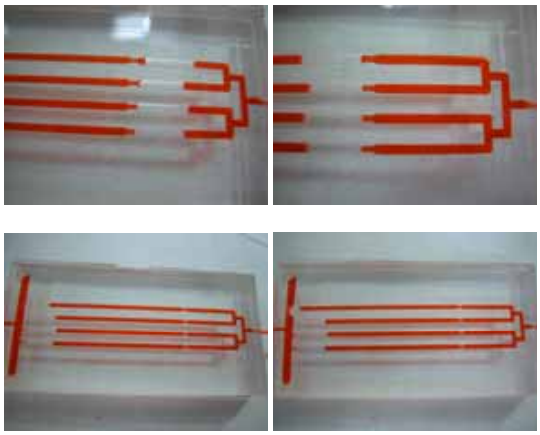

Figure 5: Photos of the bubbles moved along the channels for four consecutive times.

To demonstrate the high-throughput drug screening process, we present the similar results as shown in Fig. 6 except the blue ink which is injected into the bubbles. Figure 6 shows all the blue ink slugs progress down the channels successfully without any dilutions with the liquid water. This experiment is proceeded to simulate that the drugs flowed passing the cells coated onto the bottoms of the channels. In the future, this apparatus will serve as a tool for biochemical analyses.

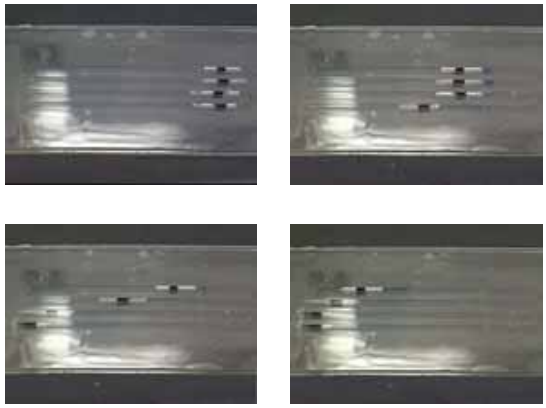

Figure 6: Photos of the blue ink slugs moved with the bubbles along the channels for four consecutive times.

5 CONCLUSIONS

In the present study, we have demonstrated the filling processes of the liquid in microfluidic chips by experimental studies. These chips comprised four channels are fabricated via mechanical milling processes. The results are presented in terms of the movement of the gas-liquid interface. During the filling processes the meniscus progression results from the overcoming of the pressure barriers which are made by an abrupt enlargement in the channel cross section. It is clear that the medium filling processes without any bubble entrapments is significantly influenced by the existence of the waste reservoir. Finally, we show the simulated high-throughput drug screening process. All the blue ink slugs progress down the channels successfully without any dilutions with the liquid water.

REFERENCES

[1] Y. Tanaka et al., "Drug Response Assay on Microchips Using Human Hepatoma Cells," Proceedings of MicroTAS 2004, Malmo, Sweden, 315, 2004.

[2] A. Puntambekar et al., "An Air-Driven Fluidic Multiplexer Integrated with Microdispensers," Proceedings of MicroTAS 2001, Monterey, CA, USA, 78, 2001.

[3] Y. Feng et al, "Passive Valves Based on Hydrophobic Microfluidics," Sensors and Actuators A, 108, 138, 2003.

[4] M. R. McNeely et al., "Hydrophobic Microfluidics," SPIE conference on Microfluidic Devices and Systems II, 3877, 210, 1999.

[5] H. Andersson et al., "Hydrophobic Valves of Plasma Deposited Octafluorocyclobutane in DRIE Channels," Sensors and Actuators B, 75, 136, 2001.

[6] P. F. Man et al., "Microfabricated Capillarity-Driven Stop Valve and Sample Injector," IEEE 11th Annual. Int. MEMS Workshop, Germany, 45, 1998.

[7] M. Lago and M. Araujo, "Threshold Pressure in Capillaries with Polygonal Cross Section," J. Colloid Interface Science, 243, 219, 2001.